COPYRIGHT NOTICE

Optimal hemoglobin extinction coefficient dataset for near-infrared spectroscopy

Yue Zhao[1#], Lina Qiu[2#], Yunlong Sun[1], Chong Huang[3], and Ting Li[1*]

[1]Institute of Biomedical Engineering, Chinese Academy of Medical Science and Peking Union Medical College, 300192, Tianjin, China
[2]Department of Physics, Politecnico di Milano, Milan, 20133, Italy
[3]Department of Biomedical Engineering, University of Kentucky, Lexington, Kentucky, USA 40506
[*]liting@uestc.edu.cn

Abstract: Extinction coefficient (ε) is a critical parameter for quantification of oxy-, deoxy-, and total-hemoglobin concentrations ($\Delta[HbO_2]$, $\Delta[Hb]$, $\Delta[tHb]$) from optical measurements of Near-infrared spectroscopy (NIRS). There are several different ε datasets which were frequently used in NIRS quantification. A previous study reported that even a small variation in ε could cause a significant difference in hemodynamic measurements. Apparently the selection of an optimal ε dataset is important for NIRS. We conducted oxygen-state-varied and blood-concentration-varied model experiments with 57 human blood samples to mimic tissue hemodynamic variations. Seven reported ε datasets were evaluated by comparisons between quantifications and assumed values. We found that the Moaveni et al (1970)' ε dataset was the optimal one, the NIRS quantification varied significantly among different ε datasets and parameter $\Delta[tHb]$ was most sensitive to ε datasets selection.

OCIS codes: (170.6510) Spectroscopy, (120.0120) Instrumentation, measurement, and metrology, (170.1470) Blood or tissue constituent monitoring

---

References and links

1. J. M. Murkin , M. Arango, "Near-infrared spectroscopy as an index of brain and tissue oxygenation," British journal of anaesthesia, **103**(suppl 1), i3-i13 (2009).
2. S. B. Colak, M. B. Van der Mark, G. W. t Hooft,, J. H. Hoogenraad, E. S.Van der Linden, F. A. Kuijpers," Clinical optical tomography and NIR spectroscopy for breast cancer detection," IEEE Journal of selected topics in quantum electronics, **5**(4), 1143-1158 (1999)..
3. D. T. Delpy and M. Cope, "Quantification in tissue near-infrared spectroscopy," Phil. Trans. Biol. Sci., **352**(1354), 649-659(2002).
4. F. F. Jöbsis, "Noninvasive, infrared monitoring of cerebral and myocardial oxygen sufficiency and circulatory parameters," Science **198**, 1264-1267 (1977).
5. G. Strangman, M. A. Franceschini, D. A. Boas, "Factors affecting the accuracy of near-infrared spectroscopy concentration calculations for focal changes in oxygenation parameters," Neuroimage **18**(4), 865-879 (2003).
6. B.L. Horecker, "The absorption spectra of hemoglobin and its derivatives in the visible and near infrared regions," J. Biol. Chem. **148**(1), 173–183, 1943.
7. J. G. Kim, H. Liu, "Variation of haemoglobin extinction coefficients can cause errors in the determination of haemoglobin concentration measured by near-infrared spectroscopy," Phys. Med. Biol. **52**(20), 6295 (2007).
8. J. G. Kim, M. Xia, H. Liu, "Extinction coefficients of hemoglobin for near-infrared spectroscopy of tissue," IEEE engineering in medicine and biology magazine **24**(2), 118-121 (2005).
9. M. Cope, "The application of near infrared spectroscopy to non invasive monitoring of cerebral oxygenation in the newborn infant," Department of Medical Physics and Bioengineering 342 (1991).
10. S. Prahl, "Tabulated molar extinction coefficient for hemoglobin in water," Oregon Medical Laser Center, 4 (1998).
11. S. Wray, M. Cope, D.T. Delpy, J.S. Wyatt, and E. Osmund R. Reynolds, "Characterization of the near infrared absorption spectra of cytochrome aa3 and haemoglobin for the non-invasive monitoring of cerebral oxygenation," Biochimica et Biophysica Acta. **933**(1), 184-192 (1988).

12. W.G. Zijlstra, A. Buursma, and W.P. MeeuwsenvanderRoest, "Absorption spectra of human fetal and adult oxyhemoglobin, de-oxyhemoglobin, carboxyhemoglobin, and methemoglobin" Clin.Chem. **37**(9), 1633-1638 (1991).
13. M. K. Moaveni, "A multiple scattering field theory applied to whole blood," Dept. of Electrical Engineering. University of Washington (1970).
14. S. Takatani, M. D. Graham, "Theoretical analysis of diffuse reflectance from a two-layer tissue model," Biomedical Engineering, IEEE Transactions on **12**, 656-664, (1979).
15. N. Kollias, W. B. Gratzer, "Tabulated molar extinction coefficient for hemoglobin in water," Wellman Laboratories, Harvard Medical School, Boston **5**, 150-161 (1999).
16. W. G. Zijlstra, A. Buursma, O. W. van Assendelft, "Visible and near infrared absorption spectra of human and animal haemoglobin: determination and application," VSP (2000).
17. T. Shiga, K. Yamamoto, K. Tanabe, Y. Nakase, B. Chance, "Study of an algorithm based on model experiments and diffusion theory for a portable tissue oximeter," J Biomed. Opt. **2**(2), 154-161(1997).
18. T. Li, M. Duan, Y. Zhao, G. Yu, Z. Ruan," Bedside monitoring of patients with shock using a portable spatially-resolved near-infrared spectroscopy," Biomed. Opt. Express **6**(9):3431-3436 (2015).
19. T. Li, Yaoxian Li, Yu Lin, and Kai Li, "Significant and sustaining elevation in blood Oxygen of Chinese cupping therapy as assessed by functional near-infrared spectroscopy," **Biomed. Opt. Express**. **8**(1), 276205, 2017.
20. H. Sato, M. Kiguchi, F. Kawaguchi, A. Maki, "Practicality of wavelength selection to improve signal-to-noise ratio in near-infrared spectroscopy," Neuroimage **21**(4), 1554-1562 (2004).
21. S. Fantini, M. FRANCESCHINIFANTINI, J. Maier, S. Walke , B. Barbieri, E. Gratton, "Frequency-domain multichannel optical detector for noninvasive tissue spectroscopy and oximetry," Opt. Eng. **34**(1), 32-42 (1995).

1. Introduction

Near infrared spectroscopy (NIRS) has been intensively developed for vivo measurements, including muscle [1], breast tumor detection [2], and functional brain imaging [3], since the seminal work of Jöbsis demonstrated the possibility of using near infrared light (~700-900 nm) to non-invasively detect tissue hemodynamics [4]. In this technique, near infrared light is utilized to illuminate tissue and the diffuse reflected light through tissue is recorded for the quantification of hemoglobin concentrations. There are three main NIRS techniques have been developed until now, including continuous-wave (CW), time-domain (TD) and frequency-domain (FD) NIRS [3]. The CW NIRS is most commonly used, which is solely based on a light intensity measurement and quantifies oxygenation changes, i.e. oxy-hemoglobin (HbO_2) and deoxy-hemoglobin (Hb) hemoglobin calculated by modified Lambert–Beer's law [5] as follows.

$$OD_\lambda = \left(\varepsilon_{HbO_2}^\lambda [HbO_2] + \varepsilon_{Hb}^\lambda [Hb] \right) \cdot DPF_\lambda \cdot d + G \qquad (1)$$

, where OD is optical density, the index λ denotes the wavelength of the light. $\varepsilon_{HbO_2}^\lambda$ and ε_{Hb}^λ are the extinction coefficients of $\Delta[HbO_2]$ and $\Delta[Hb]$ at wavelength λ, respectively; DPF is the differential path length factor, d denotes the source–detector separation and G is a factor which accounts for the measurement geometry. It clearly shows that the quantification of $\Delta[HbO_2]$ and $\Delta[Hb]$ depends on the accuracy of ε and DPF [5]. The DPF is a function of wavelength and can be measured by TD and FD techniques. Extinction coefficients of hemoglobin are also wavelength dependent and have been widely studied by laboratory spectrophotometric measurements [5-6]. The NIRS community has paid great attention on the effect of DPF [5], resulting in well-accepted and reliable methodologies. However, there are few reports about the ε effect on the accuracy of hemoglobin calculation in NIRS [7-8]. There was controversy on which ε values should be used for in-vivo NIRS considering the conventional ε values were offered mostly by in-vitro measurements [8]. It was demonstrated that variation of hemoglobin extinction coefficients can cause 5~25% relative difference in the determination of hemoglobin concentration measured by NIRS [7-8]. Apparently the optimal selection of ε values is important for NIRS quantification.

The ε dataset employed in human NIRS study are mainly from seven reported datasets, namely Cope et al (1991) [9], Prahl et al (1998) [10], Wray et al (1988) [11], Zijlstra et al [12], Moaveni (1970) [13], Tkatani et al (1979) [14] and Gratzer et al (1999) [15]. The above ε

dataset in the NIR range (700-900 nm) are plotted in Fig.1. Obviously, the 7 different sets of ε trend approximately similar, but with notable different values, especially for ε_{Hb}. Kim and Liu (2007) demonstrated that even a small variation (0.01 cm^{-1} mM^{-1}) in extinction coefficients can cause a significant difference (5~25%) in the quantification of $\Delta[HbO_2]$ and $\Delta[Hb]$ [7]. In their study, the quantification difference of hemoglobin concentrations caused by ε variations were estimated by theoretical analysis and verified by one sample experiment. The error estimation was relied on one blood sample; a robust conclusion is expected from experimental data on large number of samples. Besides, this pioneer work offered the quantification discrepancy among three reported ε datasets [10-11], while the optimal ε dataset is still unknown for NIRS quantification.
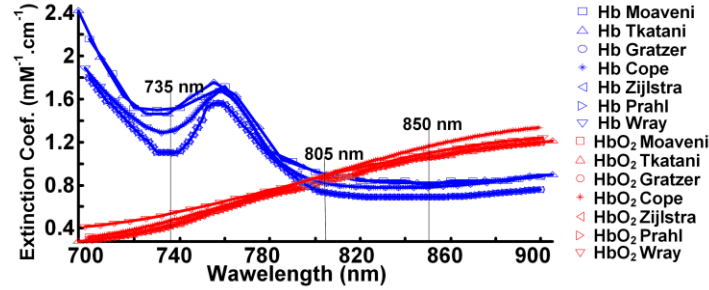

Fig.1 Absorption spectra of HbO$_2$ and Hb from Moaveni (1970), Tkatani et al (1979), Gratzer et al (1999), Cope et al (1991), Zijlstra et al (1991), Prahl et al (1998) and Wray et al (1988).

The work of this paper is to evaluate the reported 7 ε datasets, by means of varying $\Delta[HbO_2]$ and $\Delta[Hb]$ in 57 blood samples from different healthy volunteers and comparisons between quantifications and assumed values, hereby to find out the optimal sets of ε and for quantification of hemoglobin concentrations in NIRS.

2. Method and Materials

2.1 Subjects

Blood samples were obtained from 60 healthy volunteers (32 males and 28 females) who were recruited from the university community by physical check-up. The average age was 22.9 years old with no significant age difference between genders (p=0.13). No subject had taken any drugs before 5 ml blood sampling. All volunteers provided their consent to take part in our study in written form. Considering that the blood-related diseases may affect the experimental results, 1 female and 2 males were excluded through the hospital blood inspection. The presented study was approved by University of Electronic Science and Technology of China Ethnics Review Board.

2.2 Experiment setup and protocol

The experimental setup consisted of a tissue-like liquid phantom, a NIRS probe, a function module and a computer, as shown in Fig.2. The phantom [7, 17] was prepared to simulate blood content and oxygen variation in living human tissue, composed of an 8.9-cm-diameter polyethylene container with some mixture solution in it, with similar optical property with human tissue. To simulate the physiological environment of normal human, 450 ml phosphate-buffered saline (PBS) was filled into the container. 10 ml 10% intralipid solution, serving as a scatterer, was then added to the PBS. The polyethylene container was placed on the plate of a magnetic stirring apparatus to control the solution temperature at 37±1℃ during experiments, similar as the human body temperature. Followed by the deoxygenation method of Ref.17, prior to measurement, 5 g yeast (proved to be more than enough to dioxide the hemoglobin) was spread into the mixture solution. After 20 s of baseline measurement, 0.5 ml human blood was added into the solution to simulate blood content variation. Then, 99.99% oxygen gas was lead into the solution to oxygenate the hemoglobin during oxygenation state.

After the hemoglobin being fully oxygenated, the oxygen gas supply was stopped to allow oxygen to be consumed by the yeast and to induce hemoglobin deoxygenation. The same process of adding blood-oxygenation-deoxygenation, regarded as one cycle, was repeated 6 times. This same protocol was performed on 57 blood samples. All experiments were performed in a dark room.
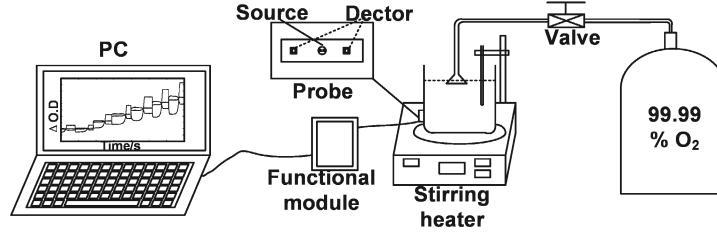

Fig. 2 Experimental setup, including a tissue-like liquid phantom, a NIRS probe (a source and a detector), a functional module and a computer.

A customized CW-NIRS system [18-19], which consisted of a probe, a functional module and a computer, was employed to record light intensity variations during experiments. The probe included a LED source with three-wavelength (735, 805, and 850 nm) and a photosensitive detector. The detector was attached on the polyethylene container with a distance 30 mm away from the source. The measured data was collected, displayed, and analyzed by a computer through a data acquisition software.

2.3 Data analysis

While three wavelengths were used, the equation (1) can be rewritten as:

$$\begin{pmatrix} \triangle \text{OD}_{\lambda_1} \\ \triangle \text{OD}_{\lambda_2} \\ \triangle \text{OD}_{\lambda_3} \end{pmatrix} = \begin{pmatrix} \varepsilon_{\text{Hb}}^{\lambda_1} & \varepsilon_{\text{HbO}_2}^{\lambda_1} \\ \varepsilon_{\text{Hb}}^{\lambda_2} & \varepsilon_{\text{HbO}_2}^{\lambda_2} \\ \varepsilon_{\text{Hb}}^{\lambda_3} & \varepsilon_{\text{HbO}_2}^{\lambda_3} \end{pmatrix} \begin{pmatrix} \triangle [\text{Hb}] \\ \triangle [\text{HbO}_2] \end{pmatrix} \cdot \text{DPF} \cdot \text{d} \tag{2}$$

, where $\varepsilon_{\text{Hb}}^{\lambda_1}$, $\varepsilon_{\text{Hb}}^{\lambda_2}$, $\varepsilon_{\text{Hb}}^{\lambda_3}$, $\varepsilon_{\text{HbO}_2}^{\lambda_1}$, $\varepsilon_{\text{HbO}_2}^{\lambda_2}$ and $\varepsilon_{\text{HbO}_2}^{\lambda_3}$ are the extinction coefficients of HbO$_2$ and Hb at wavelengths λ_1, λ_2 and λ_3 respectively, which were extracted from every reported dataset. Since the reported ε datasets were not available at every wavelength, some of them are obtained by linear interpolation. Note that DPF was assumed to be a constant for every wavelength and induced as a scaling factor here, since accurate estimation of DPF is almost impossible with continuous-wave NIRS technique [20]. This assumption will not affect the deviation comparison caused by different ε dataset [20]. Then $\Delta[\text{HbO}_2]$ and $\Delta[\text{Hb}]$ can be obtained from equation (2), as expressed in eq.(3):

$$\begin{pmatrix} \triangle [\text{Hb}] \\ \triangle [\text{HbO}_2] \end{pmatrix} = \frac{1}{\text{DPF} \cdot \text{d}} \begin{pmatrix} \varepsilon_{\text{Hb}}^{\lambda_1} & \varepsilon_{\text{HbO}_2}^{\lambda_1} \\ \varepsilon_{\text{Hb}}^{\lambda_2} & \varepsilon_{\text{HbO}_2}^{\lambda_2} \\ \varepsilon_{\text{Hb}}^{\lambda_3} & \varepsilon_{\text{HbO}_2}^{\lambda_3} \end{pmatrix}^{-1} \begin{pmatrix} \triangle \text{OD}_{\lambda_1} \\ \triangle \text{OD}_{\lambda_2} \\ \triangle \text{OD}_{\lambda_3} \end{pmatrix} \tag{3}$$

The $\Delta\text{OD}_{\lambda_i}$ was obtained by measuring light intensity under transient and baseline state respectively. Based on equation (3), the $\Delta[\text{HbO}_2]$ and $\Delta[\text{Hb}]$ were quantified by using every reported ε dataset mentioned above. Of note, the hemoglobin concentration of phantom can be justified from the volume ratio of blood to the solution during the experiment. By comparing the assumed blood concentrations with measured concentrations, the errors caused by every ε dataset can be evaluated by the following equation (4):

$$\text{Er} = \sqrt{\sum_{i=1}^{N}(\text{M}_i - \text{S})^2/\text{n}} \tag{4}$$

, where Er denotes the <mark>deviation</mark>; M is the measured hemoglobin concentration by using every reported ε dataset; S is assumed hemoglobin concentration, and n is the number of samples. <mark>The volume concentration (‰v/v) was calculated by molar concentration × molar mass / mass concentration (150 g/L).</mark>

3. Results

3.1   Experimental results

Fig.3 (a) shows an example of ΔOD trace during the whole experiment process at three wavelengths. The time traces of other blood samples were similar with the example. As can be seen from Fig.3 (a), ΔOD_{735} and ΔOD_{850} present opposite trends during both fully-oxygenated and fully-deoxygenated states, which are consistent with the known Hb and HbO_2 absorption spectra curves in NIR range. ΔOD_{805} increases at every blood adding operation (↑ 0.5ml blood), which Hb and HbO_2 absorption spectrum of the equivalent point in the concluding match at 805 nm (close to the isosbestic point).
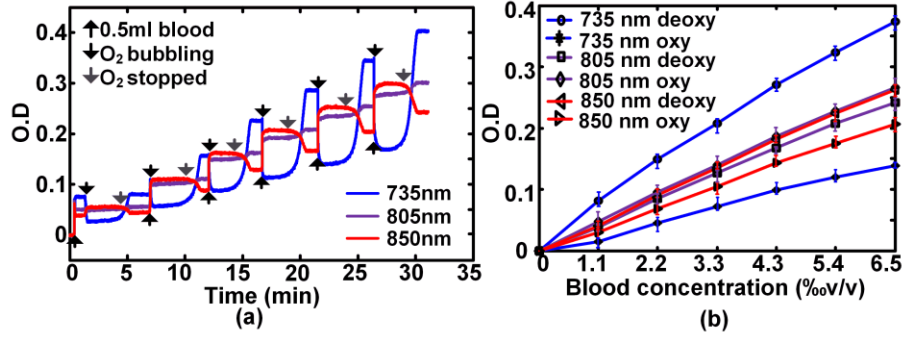

Fig.3 (a) An example of time-related ΔOD trace during the whole experiment process. The icon of ↑ 0.5ml blood denotes every blood addition; ↓ O_2 bubbling denotes the start of pump oxygen and ↓ O_2 stopped is stopping the oxygen gas. (b) <mark>The sample-averaged ΔOD with error bar on both full-oxygenated and deoxygenated states for measured wavelengths.</mark>

Fig.3 (b) <mark>shows the sample-averaged ΔOD on both full-oxygenated and full-deoxygenated states for all 57 samples.</mark> There is a linear relationship between blood concentration and ΔOD. The blood concentration after each blood addition can be known by calculating the volume ratio of the blood to the solution, which is about 1.1‰, 2.2‰, 3.3‰, 4.3‰, 5.4‰ and 6.5‰v/v ('assumed value'), respectively. On both states, ΔOD at each wavelength increased with hemoglobin concentration increment.
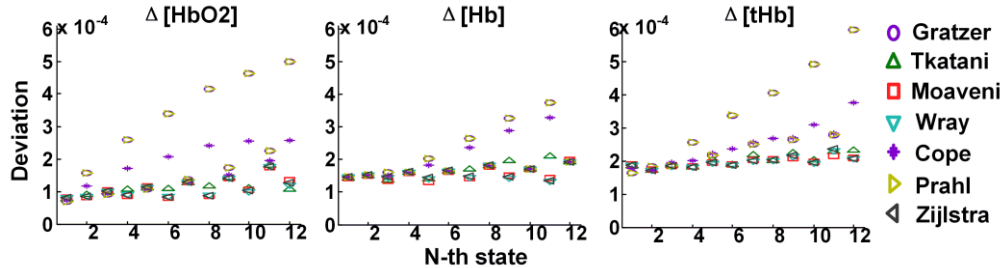
3.2 Deviation evaluation

Fig.4 The deviation evaluation of Δ[HbO₂], Δ[Hb] and Δ[tHb] caused by using 7 different ε datasets during each state. Odd states represent fully-oxygenated states and even states are fully-deoxygenated states.

Fig.4 shows deviation maps of hemodynamic parameters at N-th states between quantifications and assumed values. 'N-th state' means every full-oxygenated or

deoxygenated state, including 6 fully-oxygenated states (odd state) and 6 fully-deoxygenated states (even state). From the maps of '$\Delta[HbO_2]$', '$\Delta[Hb]$' and '$\Delta[tHb]$', we can find that the deviations caused by ε values from Gratzer (1999), Cope et al (1991) and Prahl et al (1998) are much higher than that from Tkatani et al (1979), Zijlstra et al (1991), Moaveni (1970) and Wray et al (1988). Gratzer and Prahl's are very close. Moaveni's state-averaged $\Delta[tHb]$ deviation was the minimum (≈ 0.000196), Wray's (≈ 0.000197), Zijlstra's (≈ 0.000198) and Tkatani's (≈ 0.000203) were the next. Clearly, the deviations of Tkatani, Zijlstra, Moaveni and Wray are relative smaller, and Moaveni's is the smallest. In addition, Fig.4 implied that the deviations in $\Delta[tHb]$ are always larger than those of $\Delta[HbO_2]$ and $\Delta[Hb]$, which is consistent with Fantini et al's report [21].

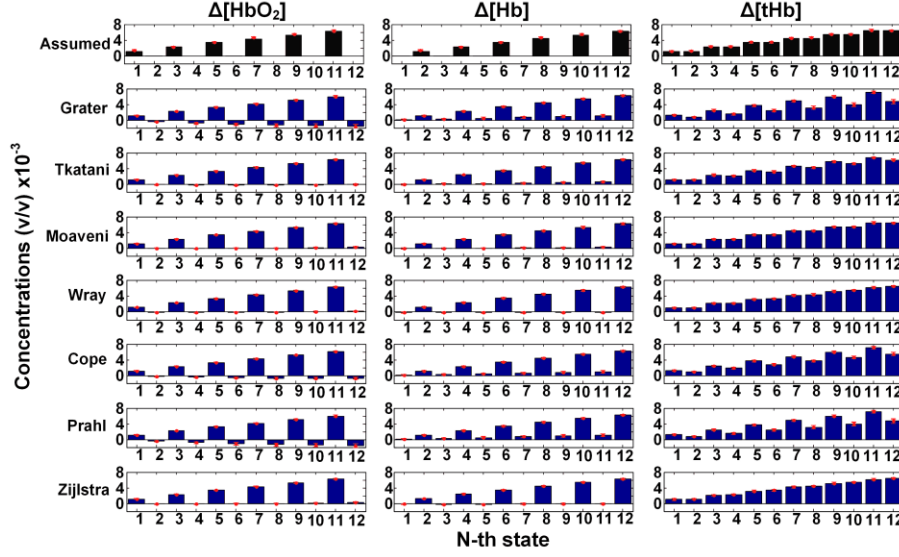**Fig.5** Sample-averaged assumed and measured hemodynamics for every state by using 7 different ε datasets, respectively. Odd-order state represents fully-oxygenated state and even-order state is fully-deoxygenated state. The standard deviation (SD) values were marked in red.

Table 1: Correlations between 7 sets of quantified and assumed values for $\Delta[HbO2]$, $\Delta[Hb]$ and $\Delta[tHb]$.

	$\Delta[HbO2]$		$\Delta[Hb]$		$\Delta[tHb]$	
	Correlation	P-value	Correlation	P-value	Correlation	P-value
Grater&Assumed	0.9845	0.0000	0.9904	0.0000	0.8998	0.0001
Tkatani&Assumed	0.9986	0.0000	0.9974	0.0000	0.9940	0.0000
Moaveni&Assumed	0.9989	0.0000	0.9986	0.0000	0.9997	0.0000
Wray&Assumed	0.9988	0.0000	0.9984	0.0000	0.9987	0.0000
Cope&Assumed	0.9944	0.0000	0.9930	0.0000	0.9567	0.0000
Prahl&Assumed	0.9844	0.0000	0.9904	0.0000	0.8995	0.0001
Zijlstra&Assumed	0.9989	0.0000	0.9983	0.0000	0.9977	0.0000

Further, we compared every quantification with assumed values in each state (Fig.5). The assumed $\Delta[HbO_2]$ rises steadily in every fully-oxygenated state (odd state) while the assumed $\Delta[Hb]$ increases every fully-deoxygenated state. The $\Delta[tHb]$ keeps constant at every same cycle of oxygenation and deoxygenation and steadily increases with blood adding procedure. Comparing between quantification and assumed values, the trend maps (Fig.5) of 'Gratzer', 'Cope' and 'Prahl' show the largest difference. And the trend of 'Tkatani' is either unreasonable, because the $\Delta[tHb]$ didn't keep constant during every same cycle. By contrast, the trends of 'Zijlstra', 'Moaveni' and 'Wray' are very close to the assumed values. The maximum SD of mean OD is 5.7%, which shows the high quality of the collected data. In

Here the direct comparison of hemoglobin concentrations is not meaningful, because DPF was induced as a scaling factor when calculating the measured concentrations. Hereby, based on Fig.5 only, it is difficult to determine the optimal one among 'Zijlstra', 'Moaveni' and 'Wray'.
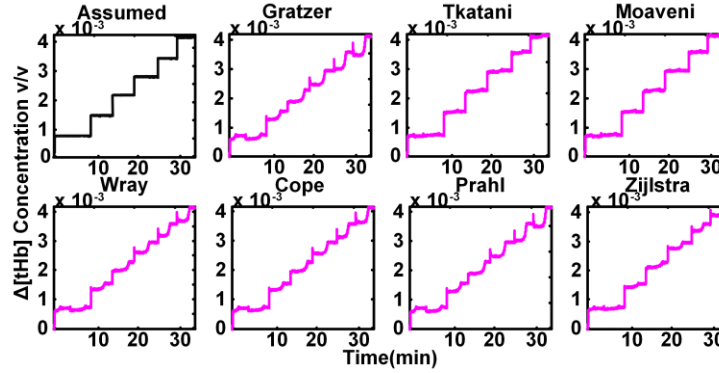

Fig.6 Time responses of assumed and measured $\Delta[tHb]$ variations.

To find the optimal ε dataset among Zijlstra's, Moaveni's, and Wray's, we further compared the time response of quantified and assumed values. As mentioned, $\Delta[tHb]$ concentration was expected to be the same as $\Delta[HbO_2]$ on fully-oxygenated state and $\Delta[Hb]$ on fully-deoxygenated state, hereby we only show the result of $\Delta[tHb]$. Fig.6 showed that the time response trend of 'Moaveni' is closest to the assumed values among the three candidates. Above all, it is no doubt that the ε dataset of Moaveni et al (1970) is the optimal among the reported ε datasets.

4．Discussion and conclusion

The extinction coefficient ε is an important parameter for quantifying hemoglobin concentration and oxygen saturation in biological tissues using NIRS. Based on a preliminary research showing that variations in ε values might induce 5~25% relative difference in NIRS quantifications, we attempt to pick up an optimal ε dataset for NIRS quantification of hemodynamic parameters from the reported seven different ε datasets which have been frequently used by NIRS community all over the world.

We conducted oxygen-state-varied blood model experiments with 57 human blood samples to stimulate the oxygen consumption in human tissue. By comparing with the assumed blood concentrations by these tissue-like liquid phantoms, the discrepancies (deviation) between the quantifications of $\Delta[HbO_2]$, $\Delta[Hb]$ and $\Delta[tHb]$ by using 7 different ε datasets and the assumed values were evaluated. The assumed values were obtained from the volume ratio of blood to the solution on oxygenated and deoxygenated states. The preliminary work [7, 8] used only a single blood sample in experiment to show the significant variation induced by 3 different ε datasets. Here we recruited 57 subjects to collect 57 blood samples, and performed experiments on each blood samples. With the data statistical analysis on population, it's more convincing to conclude the quantitative differences in quantification induced by different ε datasets. Plus, our experiment design included repeated circles of adding blood- full oxygenation-full deoxygenation, allowing us to obtain the assumed values of $\Delta[HbO_2]$, $\Delta[Hb]$ and $\Delta[tHb]$ at fully oxy- and deoxy-genated states and to use these values to testify the quantifications using those seven ε datasets respectively.

We focused on the effect of different ε dataset for NIRS quantification and intended to figure out the optimal one for human NIRS study. Our results showed that different ε dataset caused significant difference in quantification of hemoglobin concentrations, which is

consistent with the result of Kim and Liu (2007). For the deviation evaluation, we found that deviations in quantification caused by using ε values from Gratzer (1999), Cope et al (1991) and Prahl et al (1998) were much larger than that from Tkatani et al (1979), Zijlstra et al (1991), Moaveni (1970) and Wray et al (1988). The most accurate quantification was obtained in case of using ε values provided by Moaveni (1970). Moreover, our results (Fig.4 and Fig.5) also showed that the deviation of $\Delta[tHb]$ is always higher than those of $\Delta[HbO_2]$ and $\Delta[Hb]$. This observation agrees with the results in the report of Fantini et al [21], which indicates that the quantification of blood volume is the most sensitive to selection of ε dataset or variations in ε. Our findings enhanced the pioneer work on the effect of ε variation on NIRS quantification [7, 8] by a large population data and took an important pace forward to quantitatively recommend an optimal ε dataset for NIRS community.

In our study, we focused on the effect of ε dataset on NIRS quantification, but not DPF which was assumed to be a constant and equal at all three used wavelengths in our quantifications. Basically, DPF was a scaling factor here which would not affect the deviation analysis induced by variations of extinction coefficients. However, the comparisons of the effects between ε dataset difference and DPF variation are meaningful to get a more complete view of impact factors in NIRS quantifications. The bandwidth of the three wavelengths are as small as 10 nm, which affects little to the OD curve. The main limitation of this study would be the Asians-only and age-concentrated (17~33 years old) sample. Further study should regard any racial or age-related difference in ε values.

In summary, this study extensively evaluated seven ε datasets reported by various groups through varying the concentrations of oxy- and deoxy-hemoglobin in blood samples from 57 healthy volunteers. The data of the population strongly convinced us the significant discrepancy in NIRS quantification caused by different ε datasets and pointed out $\Delta[Hb]$ is most sensitive to ε difference. More importantly, we successfully found that the ε dataset provided by Moaveni (1970) is the optimal in the quantification of hemodynamics in NIRS field.

Disclosures

The authors declare that there are no conflicts of interest related to this article.